

A novel approach to assess the dynamics of extra-chromosomal circular ribosomal DNA in human cells

Joerg Leheste, Emily Forbes, Kristin DiGregorio, Victoria Katz, Alyssa Miceli, Christopher Husko, Raddy L Ramos, German Torres

Several nutrient-signaling pathways that extend life span have been described in model organisms. Thus, parallel and redundant signaling pathways that are similar across species might be subject to experimental manipulation. Here, we develop a PCR-based technique for testing the hypothesis that mitotic accumulation of extra-chromosomal ribosomal DNA circles might also determine life span in human cells. Using resveratrol, a phytochemical that counters age-related signs, we find treatment-dependent subcellular accumulations of extra-chromosomal 5S ribosomal DNA in human cell lines. These data suggest an association between DNA circles and intrinsic aging and demonstrate the utility of a PCR-based technique for studying the accumulation of dysfunctional molecules that promote senescence.

1 **Authors**

2 **Joerg R. Leheste¹⁺, Emily Forbes¹, Kristin DiGregorio¹, Victoria Katz¹, Alyssa**
3 **Miceli¹, Christopher Husko¹, Raddy L. Ramos¹, German Torres¹**

4 ¹ Department of Biomedical Sciences
5 New York Institute of Technology College of Osteopathic Medicine
6 Northern Boulevard
7 P.O. Box 8000
8 Old Westbury, NY 11568-8000
9 USA

10 * Corresponding author Joerg R. Leheste
11 Phone: (001) 516-686-3764
12 Fax: (001) 516-686-1454
13 E-mail: jleheste@nyit.edu

14 1. Introduction

15 Aging appears to be plastic and can be manipulated by genetic and nutritional
16 intervention. For example, activation of the silent information regulator T1 (SIRT1)
17 pathway increases the life span of model organisms such as yeast and mice. SIRT1 is a
18 NAD⁺-dependent deacetylase that directly links transcriptional regulation to intracellular
19 metabolism (Howitz et al., 2003). Among the signaling cues that activate SIRT1
20 pathways is the polyphenol molecule, resveratrol. SIRT1 activation by resveratrol
21 triggers a broad range of transcription factors and co-regulators that mediate key
22 mechanisms in the cell cycle, cell growth and apoptotic and autophagic programs of cell
23 death (Baur, 2010; Torres et al., 2008; Torres et al., 2011). Other intracellular
24 mechanisms activated by SIRT1-dependent pathways are those related to DNA stability
25 and DNA replication. For example, using the budding yeast (*Saccharomyces cerevisiae*)
26 as a model for elucidating signaling pathways that control life span, Sinclair and
27 Guarente (1997) showed that increased activity of SIR2 (the yeast ortholog of
28 mammalian SIRT1) suppresses the gradual accumulation of extra-chromosomal circular
29 DNA (eccDNA). As its name implies, eccDNA are circular molecules propagated extra-
30 chromosomally from repetitive and non-repetitive genomic regions of various species
31 including, humans (Cohen and Segal, 2009; Cohen et al, 2010; Flores et al., 1988;
32 Meyerink et al. 1979).

33 As in yeast, human ribosomal DNA (rDNA) is also organized in tandem rDNA
34 repeats with five 43 kb rDNA (*rna45s5*) clusters encoding a large 45S rRNA precursor
35 that is post-transcriptionally processed into 28S, 18S and 5.8S rRNAs (Henderson et al.,
36 1972; Gonzalez and Sylvester, 1995). 5S rRNA is encoded by a separate 5S rDNA
37 (*rna5s1*) cluster with 100-150 copies of a 2.2kb rDNA tandem repeat (Little and Braaten,
38 1989; Sorensen and Frederiksen, 1991). Investigations into the genomic architecture of
39 human rDNA clusters reveal significant meiotic re-arrangement of about 11% per
40 generation per gene cluster (Strults et al., 2008), with 5SrDNA molecules undergoing
41 significant replicative steps (Cohen et al., 2010). In humans, SIRT1 expression is also
42 associated with rDNA re-arrangements suggesting a conserved composition and
43 function of anti-aging pathways. However, there is little experimental evidence for these
44 association pathways, in particular whether activation of SIRT1 or reduction of eccrDNA
45 could be considered for the prevention of specific diseases. In addition, there is no
46 sensitive platform for functional screening of human eccrDNA which allows for the
47 precise and accurate analysis underlying the formation of eccrDNA molecules. To
48 address this technical limitation, we developed and validated a PCR-based protocol in
49 combination with a nuclear transport assay for the quantitative analysis of eccrDNA
50 molecules. To further support its practical use, we tested whether this technique could
51 identify the occurrence of additional eccDNA species in human cell lines.

52

53 2. Materials & Methods

54 2.1 Cell Culture, Drug Treatment and Collection of Human Cells

55 The following adherent human epithelial cell lines were grown under standard
56 culture conditions at 37°C with 5% CO₂: HEK-293 (embryonic kidney, CRL-1673); SH-
57 SY5Y (neuroblastoma, CRL-2266) and; MCF7 (mammary adenocarcinoma, HTB-22),
58 (ATCC, VA, USA). HEK-293 and MCF7 cells were grown in Dulbecco's Modified Eagle
59 Medium (DMEM) and SH-SY5Y in a 1:1 mixture of Eagle's Minimum Essential Medium
60 (EMEM), and F12 Medium. Additionally, all media were supplemented with 10% fetal
61 bovine serum, 1% penicillin/streptomycin, 1% glutamine (Glutamax), 1% anti-mycotic
62 (Fungizone) and 1% non-essential amino acids. Cells were propagated 1:10 using
63 0.25% (w/v) Trypsin/0.53 mM EDTA upon reaching a cellular density of approximately
64 70% - 80% (tissue culture reagents and supplements: Invitrogen, Carlsbad, CA, USA).
65 Experiments were conducted with cells on standard 6-well multi-well plates. Resveratrol
66 was dissolved in DMSO at a concentration of 100 mM, aliquotted and stored in light-
67 proof containers at - 20 °C. Resveratrol treatment (50 µM, final concentration), was
68 initiated at a cellular confluence level of about 70% for 6h or 48h. For nuclear transport
69 studies, the lectin wheat germ agglutinin (WGA) was used to block nuclear transport (0.1
70 mg/ml, final concentration; 12h) and the lectin concavalin A (ConA) as control (0.1
71 mg/ml, final concentration; 12h). At the end of a given treatment period, cells were
72 washed with 1X PBS, scraped off their dishes and collected by centrifugation for further
73 analysis or stored at -80 °C.

74 2.2 Resveratrol-dependent Changes in Gene Expression using Quantitative PCR 75 (QPCR)

76 Following 48h of resveratrol-treatment of human cells (HEK-293, MCF7, SH-
77 SY5Y) on multi-well dishes, cells were collected and total RNA was prepared using the
78 RNeasy RNA-isolation system/Qia shredder according to the manufacturer's
79 specifications (Qiagen, Valencia, CA, USA) and as previously described by our group
80 (Torres et al., 2008). RNA concentrations and integrity were determined *via* standard
81 spectrophotometry and agarose gel-electrophoresis. Reverse transcription of RNA into
82 complementary cDNA was carried out with the Superscript III First Strand Synthesis
83 System for RT PCR (Invitrogen, Carlsbad, CA, USA). QPCR was conducted on a
84 Mastercycler ep gradient S (Eppendorf AG, Hamburg, Germany) using Power SYBR
85 Green PCR Master Mix (Applied Biosystems, Foster City, CA, USA) with a total volume
86 for each sample of 20 µl. Gene-specific DNA primers were either used as previously
87 reported (Murayama et al., 2008) or designed using the integrated DNA Technologies
88 Primer Quest tool (IDT, Coralville, IA, USA). Expression was accessed for *sirt1*, *rn5s1*
89 (5SrRNA) and *rna45s5* (45S pre-ribosomal RNA) using the following primers: *β-actin*
90 forward: 5'-CAG CCA TGT ACG TTG CTA TCC AGG-3'; *β-actin* reverse: 5'-AGG TCC
91 AGA CGC AGG ATG GCA TG-3'; *rn5s1* forward: 5'-GAT CTC GTC TGA TCT CGG AAG
92 CTA AG-3'; *rn5s1* reverse: 5'-AAA GCC TAC AGC ACC CGG TAT T-3'; *rna45s5* forward:
93 5'-GAA CGG TGG TGT GTC GTT C-3' *rna45s5* reverse: 5'-GCG TCT CGT CTC GTC

94 TCA CT-3'; *sirt1* forward: 5'-CTG TAG ACT TCC CAG ATC TTC CAG-3'; *sirt1* reverse:
95 5'-GTG ACA GAG AGA TGG CTG GAA TTG-3'.

96 **2.3 Extraction of total eccDNA and Relative Quantification of eccDNA Circles** 97 **using QPCR**

98 Resveratrol-treated HEK-293, MCF7 and SH-SY5Y cells and DMSO (solvent)
99 controls were separated into their nuclear and cytoplasmic fractions according to the
100 manufacturer's instructions (CellLytic Nuclear Extraction Kit, Sigma, St. Louis, MO,
101 USA). Both fractions were exposed to standard Na-acetate/ethanol precipitation and
102 carefully re-suspended in 100 µl TE buffer. To eliminate DNA chromosomes and linear
103 fragments, individual samples were purified with the MinElute Reaction Cleanup Kit
104 (Qiagen, Valencia, CA, USA). Then, samples were sequentially treated with
105 exonuclease III (20U/µl, 1h, 37°C), RNase A (50 µg/ml, 30 min, 37°C) and proteinase K
106 (100µg/ml, 1h, 37°C) followed by another MinElute Reaction Cleanup purification and a
107 final elution in 20 µl of a 10 mM Tris buffer, pH 8.5. QPCR was carried out as described
108 above with the same DNA primer pairs for *m5s1* and *ma45s5* only this time measured
109 against *sstI* satellite and *alu* repeats (Cohen et al., 2010): *sstI* forward: 5'-GTG GTG
110 GTG CAT GGC CCC C-3'; *sstI* reverse: 5'-GAG CTC CAG GAT CAC CAC AGC-3'; *alu*
111 forward: 5'-GGC GGG CGG ATC ACG AGG TCA G-3'; *alu* reverse: 5'-CCC GGG TTC
112 ATG CCA TTC TCC TG-3'.

113 **2.4 Isolation and PCR-amplification of Nuclear and Cytoplasmic eccDNA**

114 For the isolation of eccDNA, HEK-293 cells were grown to confluence on 6-well
115 multi-well plates and then separated into nuclear and cytoplasmic fractions with the
116 CellLytic Nuclear Extraction Kit (Sigma, St. Louis, MO, USA) followed by Na-
117 acetate/ethanol precipitation as described above. All samples were sequentially purified
118 and enzymatically treated with exonuclease III, RNase A and proteinase K as previously
119 described. To linearize 5SrDNA circles (there is a single BamHI restriction site) one half
120 of each sample (10 µl) was treated with BamHI for 4h, 37°C while the other half was
121 sonicated 3 times with 10s pulses on wet ice (30% maximum power, 2mm tip; Cell
122 Disruptor, Heat-Systems Ultrasonics, Plainview, NY, USA). Samples were then purified
123 using the MinElute Reaction Cleanup Kit (see above) and eluted in a final volume of 10
124 µl. To generate blunt ends, samples were treated with T4-DNA polymerase and dNTPs
125 (Roche Applied Science, Indianapolis, IN, USA) for 20 min at 16°C and immediately
126 purified with the MinElute Reaction Cleanup Kit. EcoRI adaptor oligonucleotides were
127 ligated to the linearized and blunt-ended DNA pieces for 18h at 16°C and excess
128 adaptors subsequently removed by gel filtration using Sephacryl S-400 spin columns
129 according to the manufacturer's instructions (both: Universal Riboclone cDNA Synthesis
130 System, Promega, Madison, WI, USA). Derivatives of eccDNA were then amplified using
131 a high fidelity PCR system (Expand 20 kb plus PCR System, Roche Applied Science,
132 Mannheim, Germany) and DNA primer matching the EcoRI adaptor sequence (forward
133 and reverse primer: AAT TCC GTT GCT GTC G; Promega, Madison, WI, USA).

134 Reactions destined for DNA cloning and sequencing were exclusively recruited from the
135 sonicated samples and subject to PCR elongation reactions at 4 min. Reactions used for
136 Southernblot analysis were recruited from sonicated as well as BamHI restricted
137 samples and subject to 15 min PCR elongation reactions.

138 **2.5 Southern blot Analysis of eccDNA**

139 Linearized and amplified eccDNA samples were slowly spread on ethidium
140 bromide-stained 0.8% agarose gels (20-30mA). Then, gels were bathed in 0.25M HCl
141 for 15min followed by transfer solution (0.5 M NaOH, 1.5 M NaCl) for 30 min before
142 being assembled for alkaline upward DNA transfer onto a BrightStar-Plus nylon
143 membrane (Ambion/Life Technologies, Carlsbad, CA, USA) with transfer solution for 12-
144 18h. After a 5 min-bath in neutralizing solution (0.5 M Tris•CL, pH8.0), the membranes
145 were dried and baked at 80 °C between blotting paper for 3h. Then, blots were pre-
146 hybridized with UltraHyb solution (Ambion/Life Technologies, Carlsbad, CA, USA) at
147 42°C for 30min and then hybridized for 12-16h with a PCR-generated and gel-extracted
148 DNA probe specific for rDNA (Strults et al., 2008) labeled using the BrightStar Psolaren-
149 Biotin System (Ambion/Life Technologies, Carlsbad, CA, USA). For signal evaluation,
150 autoradiographs were scanned and images imported into Adobe Photoshop CS5.1
151 (Adobe Systems Incorporated, Mountain View, CA).

152 **2.6 Identification and Screening of eccDNA in HEK-293 Cells**

153 Linearized and amplified eccDNA samples were briefly separated on ethidium
154 bromide-stained 1.5% agarose gels from which a fragment cluster ranging from
155 approximately 100 bp – 4kb was removed using the QIAquick Gel Extraction Kit
156 (Qiagen,Valencia, CA, USA). Purified DNA was ligated into the pGEM-T Easy vector
157 system (Promega, Madison, WI, USA) and transformed into chemically competent *E.*
158 *coli* DH5α (Invitrogen/Life Technologies, Carlsbad, CA, USA). Plasmid DNA from
159 ampicillin-resistant and beta-galactosidase negative trans-formants (blue-white
160 screening) was treated with EcoRI restriction endonuclease for 1h at 37°C and analyzed
161 via standard agarose gel electrophoresis (1.5%) to confirm presence of an insert. Only
162 confirmed clones were selected for DNA sequencing using standard T7 sequencing
163 primer (T7 RNA polymerase promoter). DNA sequences were screened for identity and
164 genomic origin with the “Basic Local Alignment Search Tool” (BLAST;
165 <http://www.ncbi.nlm.nih.gov/blast/>). To determine a potential driving-force for eccDNA
166 mobilization, all confirmed sequences were analyzed with the repetitive sequence
167 screening tool CENSOR (Kohany et al. 2006; <http://www.girinst.org/censor/index.php>).

168 **3. Results and Discussion**

169 While yeast SIR2 has a stabilizing effect on the organism’s rDNA locus, the exact
170 role of SIRT1 on human eccrDNA dynamics is unknown. In line with our previous
171 findings demonstrating a close association of SIRT1 with specific human DNA targets

172 (Torres et al., 2008; Torres et al., 2011), SIRT1 has been linked to the transcriptional
173 regulation of rna45s5 by the energy-sensing eNoSC protein complex (Murayama et al.,
174 2008; Song et al., 2013). In order to understand the epigenetic regulation of rn5s1, we
175 determined the transcriptional activity of rn5s1 and rna45s5, as well as sirt1, in HEK-293
176 cells following resveratrol treatment for 48h (Fig. 1A). Consistent with our previous work,
177 we found that the transcriptional activity of sirt1 increased by 1.9-fold ($P = 5 \times 10^{-6}$), while
178 expression of rn5s1 increased by 3.5 fold ($P = 0.02$) and rna45s5 by 1.8 fold ($P = 0.03$).
179 Parallel experiments in MCF7 and SH-SY5Y cells showed similar outcome trends, but
180 failed to reach statistical significance at the $P < 0.05$ level (data not shown). Whereas
181 expression of rn5s1 has not been studied in this context, the expressional increase at
182 rna45s5 loci is not consistent with findings related to the eNoSC protein complex, which
183 is associated with heterochromatin formation and transcriptional repression (Murayama
184 et al., 2008). This discrepancy may be related to the fact that Murayama's group
185 manipulated the nucleomethylin component of the eNoSC protein complex, whereas we
186 manipulated SIRT1 through resveratrol treatment. It should be noted, however, that it is
187 not clear what the cellular dynamics are between SIRT1 and rna45s5 or rn5s1 in human
188 cells. In gain-of-function mouse models of disease, over-expression of SIRT1 increases
189 homologous recombination of the entire rodent genome (Palacios et al., 2010). This
190 suggests that DNA stability/mobility depends, in part, on the activation of SIRT1-
191 dependent protein complexes and signaling pathways, particularly in those cells
192 involved in nutrient metabolism and cellular growth.

193 Due to the low abundance of human eccrDNAs, we sought to develop a
194 quantitative PCR-based approach for maximizing eccrDNA content. Investigations into
195 appropriate internal standards for linearized eccDNA molecules revealed human SstI
196 satellite repeats as well as Alu repeats as potential candidates. The SstI family consists
197 of 2.5 kb repeating units with approximately 400 copies within genomic clusters (Epstein
198 et al., 1987). Alu repeats are approximately 280bp long and are the most common
199 repetitive element with about 1 million copies per haploid genome. Their average
200 genomic separation of only about 3 kb increases their potential for genomic re-
201 arrangement and eccDNA formation in mammalian cells. Such non-tandem repeats
202 have previously been detected in eccDNA pools of human cells (Jones & Potter 1985;
203 Riabowol et al., 1985). As noted earlier, however, comprehensive characterization of
204 eccDNAs has been severely hampered due to their relatively low abundance in human
205 cells and tissues (Cohen et al., 2010), and the lack of convenient and high-throughput
206 readout. When comparing Alu-eccDNA or SstI-eccDNA to β -actin expression in HEK-293
207 cells using our novel eccDNA isolation/cloning strategy in conjunction with quantitative
208 PCR (QPCR), we reliably detected robust levels of Alu-eccDNA across cellular
209 compartments, whereas nuclear SstI-eccDNA was detectable in most cases but rarely in
210 the cytoplasm (data not shown). To ensure that the internal standard was unaffected by
211 our independent variable, resveratrol-treated cells (50 μ M in culture medium) and
212 controls were separated into their cytoplasmic and nuclear fractions and processed to

213 isolate eccDNA and cDNA (via reverse transcription of RNA). Comparing Alu-eccDNA
214 concentration against β -actin expression of the same cells resulted in a relative Alu-
215 eccDNA index which was independently derived for resveratrol-treated and -untreated
216 cells. We found that resveratrol treatment did not significantly affect the concentration of
217 Alu-eccDNA in either the nuclear or cytoplasmic compartment (Fig. 1B). We therefore
218 continued using Alu-eccDNA as an internal standard in subsequent experiments.

219 Next, we tested if resveratrol-dependent SIRT1 activation, which had caused
220 significant transcriptional increases at both types of rDNA loci, could also trigger
221 concomitant changes in the concentration of cellular eccrDNA from the aforementioned
222 loci (Fig. 2A-C). For this experiment, we used either total nuclear or cytoplasmic eccDNA
223 for QPCR with primers specific for rn5s1, rna45s5, and the Alu consensus sequence. In
224 HEK-293, MCF7 and SH-SY5Y cells, the abundance of rn5s1-eccrDNA in the
225 cytoplasmic fraction consistently increased by 2.2-fold ($P = 0.01$), 3.4-fold ($P = 0.002$)
226 and 1.5-fold ($P = 0.048$), respectively. At the same time, we found that rn5s1-eccDNA in
227 the nuclear fraction of HEK-293 cells was significantly decreased by about 60% ($P =$
228 0.01), but unaffected in the nuclear compartment of MCF7 and SH-SY5Y cells. Changes
229 in rna45s5-eccrDNA were not statistically significant under any experimental condition
230 (data not shown).

231 To independently confirm the presence of rn5s1-eccrDNA in HEK-293 cells, we
232 analyzed subcellular eccDNA extracts amplified with long-range PCR through Southern-
233 blot analysis (Fig. 2D) using a previously published and labeled rn5s1-eccrDNA probe
234 for detection (Strults et al., 2008; Cohen et al., 2010). Initially in this process, the
235 eccDNA samples had either been sonicated or treated with BamHI restriction
236 endonuclease (rn5s1-eccrDNA has a unique BamHI restriction site) to open up circular
237 DNA. All samples showed a hybridization signal in the 2.2 kb range which is consistent
238 with the published length of one rn5s1-eccrDNA monomer (Little & Braaten, 1989).
239 Cytoplasmic but not nuclear samples displayed an additional signal in the higher DNA
240 fragment size range at approximately 12 kb. Due to an initial filtration step, such large
241 DNA piece could have been only extracted if they were supercoiled or otherwise
242 condensed. However, the specificity of the signal indicates multicopy rn5s1eccDNA
243 which could result from recombination-dependent concatemeric rn5s1eccrDNA
244 replication as previously described in *Drosophila* (Cohen et al., 2005). Both, the
245 resistance to full BamHI restriction and cytoplasm-specific location of higher-order
246 rn5s1-eccrDNA need to be addressed in future studies.

247 To further investigate the observed resveratrol-induced cytoplasmic rn5s1-
248 eccrDNA increase in HEK-293 cells, we sought to distinguish between nuclear import
249 and cytoplasmic replication. We thus implemented a 12h treatment regimen involving
250 combinations of resveratrol (50 μ M) and WGA (0.1mg/ml) to block nuclear transport, and
251 control lectin ConA (0.1mg/ml) (Fig. 3 A, B). In cytoplasmic fractions, we confirmed an

252 average increase of 180% for rn5s1-eccDNA (P = 0.01) and 100% (P = 0.01) above
253 control levels with resveratrol alone and in combination with ConA, respectively. WGA
254 alone significantly reduced cytoplasmic rn5s1-eccrDNA to about 50% (P = 0.03) of
255 control levels, whereas WGA in combination with resveratrol restored levels to 80%
256 baseline. Resveratrol treatment without ConA depleted nuclear rn5s1-eccrDNA
257 significantly to about 30% (P = 0.01) of the control baseline. Treatment with WGA or
258 WGA in combination with resveratrol resulted in rescue frequencies of between 70%-
259 80% which were, however, not statistically significant. These results indicate transport of
260 rn5s1-eccrDNA across the nuclear envelope but do not rule out compound tributaries,
261 such as cytoplasmic rn5s1-eccDNA amplification which needs yet to be investigated.

262 While testing our novel isolation protocol in combination with standard
263 recombinant DNA technology, we were able to capture and analyze 48 eccDNA
264 molecules ranging from 420 bp to 870 bp (average: 636 bp). We traced eccDNAs to
265 chromosomes 1, 2, 4, 5, 6, 8, 9, 11, 12, 13, 14, 17, 20, X (HEK-293 cells are female)
266 without showing any particular prevalence and only 1 duplication. Sequence analysis
267 revealed that the majority of eccDNA came from unique, non-repetitive genomic loci
268 (Fig. 4). Three of the identified sequences originated from tandemly arranged gene
269 clusters: 5S rDNA (rn5S1) with an average copy number of 98 repeats (Stults et al.,
270 2007) and, once again, adding validity to our QPCR findings; protocadherin- α (pcdh α 1)
271 with 15 repeats (Wu and Maniatis, 1999) and sperm protein 4 associated with the
272 nucleus on the X chromosome (spanx4) with 5 repeats (Kouprina et al., 2004). A total of
273 3 sequences were mitochondrial. The majority of the 45 non-mitochondrial sequences
274 (30) were intergenic, 12 mapped to intron/regulatory region boundaries and 3 to coding
275 exon/intron boundaries. The identity and characteristics of all 16 eccDNAs mapping to
276 specific genes, including rn5s1 (~300 bp upstream of transcriptional start site), are
277 summarized (Tab. 1). Through further analysis with the repetitive DNA sequence mining
278 tool CENSOR (Kohany et al., 2006), we found that the majority of the 33 genomic
279 sequences (31 unique; 2 tandem repeats) included 1-4 short repetitive DNA elements
280 (1.7 on average) of which 91% are defined as transposable elements and 9%
281 interspersed DNA repeats (aluS, aluJ). Of the transposable elements, 94% were class-I
282 retrotransposons, including long interspersed nuclear elements (LINEs; includes I1),
283 short interspersed nuclear elements (SINEs; most abundant class in mammals; includes
284 aluJb, aluJo, aluSc) and endogenous retroviruses (erv1, erv2). Only 6% were class-II
285 non-autonomous DNA transposons (hAT superfamily). We believe that the abundance of
286 these elements in the genome could contribute to the formation and mobilization of
287 eccDNA via homologous recombination (Smit, 1999). The 3 eccDNA clones that
288 overlapped with actual coding exons did not include any such repetitive DNA elements
289 and therefore belong to the recently discovered class of microDNAs (Shibata et al.,
290 2012). There is a possibility, that the identified eccDNAs are byproducts of discontinuous
291 lagging strand synthesis during replication. Shibata and colleagues (Shibata et al.,
292 2012), however, were able to link the formation of certain microDNAs with corresponding
293 micro-deletions making a case for excision from the genome. The finding of rn5S1 and

294 other tandemly arranged genes in our eccDNA isolates is in line with our newly-
295 developed QPCR-based approach and in line with our Southern blot findings. The
296 abundance of interspersed repeats and transposons is suggestive of an involvement in
297 the mobilization of eccDNAs. This and their potential involvement in genetic mosaics
298 and partial aneuploidy need to be investigated in subsequent studies. The confirmation
299 of microDNAs in human eccDNA pools opens the possibilities of studying these
300 molecules using our experimental protocols.

301 **4. Conclusions**

302 There are several competing hypotheses about human aging, the inevitability of
303 death and underlying cellular and molecular mechanisms. Here, we are introducing a
304 novel PCR-based approach with cultured human cells and reveal the subcellular
305 dynamics of rn5s1-eccrDNA in response to resveratrol with important analogies to an
306 aging paradigm involving eccDNA accumulation in yeast. These findings point to rn5s1-
307 eccrDNA as a potential candidate in the search for a stimulus factor that regulates age-
308 related maintenance of telomeres and other genomic mechanisms responsible for
309 organismic senescence and death and also points to the possibility of using rn5s1-
310 eccrDNA as therapeutic target for the treatment of age-related pathologies. The
311 unexpected finding of other eccDNA molecules, such as the recently discovered class of
312 microDNAs, emphasizes the dynamics of the human genome which may bring benefits
313 to some DNA loci but detrimental damage others.

314 **5. Acknowledgements**

315 We thank all of our students and colleagues for their critical discussion of the
316 project. This work was supported by intramural funding to Joerg R. Leheste.

317 **6. References**

- 318 • Baur JA, Chen D, Chini EN, Chua K, Cohen HY, de Cabo R, Deng C, Dimmeler S,
319 Gius D, Guarente LP, Helfand SL, Imai S, Itoh H, Kadowaki T, Koya D,
320 Leeuwenburgh C, McBurney M, Nabeshima Y, Neri C, Oberdoerffer P, et al. 2010.
321 Dietary restriction: standing up for sirtuins. *Science* 2010 329: 1012-3.
- 322 • Buck SW, Sandmeier JJ, Smith JS .2002. RNA polymerase I propagates
323 unidirectional spreading of rDNA silent chromatin. *Cell* 111: 1003-14.
- 324 • Cockell MM, Perrod S, Gasser SM. 2000. Analysis of sir2p domains required for
325 rDNA and telomeric silencing in *saccharomyces cerevisiae*. *Genetics* 155: 2021.

- 326 • Cohen S, Agmon N, Yacobi K, Mislovati M, Segal D. 2005. Evidence for rolling circle
327 replication of tandem genes in *Drosophila*. *Nucleic Acids Res* 33: 4519-26.
- 328 • Cohen S, Agmon N, Sobol O, Segal D. 2010. Extrachromosomal circles of satellite
329 repeats and 5S ribosomal DNA in human cells. *Mob DNA* 1:11.
- 330 • Cohen S, Segal D. 2009. Extrachromosomal circular DNA in eukaryotes: possible
331 involvement in the plasticity of tandem repeats. *Cytogenet Genome Res* 124: 327-
332 38.
- 333 • Colman RJ, Anderson RM, Johnson SC, Kastman EK, Kosmatka KJ, Beasley TM,
334 Allison DB, Cruzen C, Simmons HA, Kemnitz JW, Weindruch R. 2009. Caloric
335 restriction delays disease onset and mortality in rhesus monkeys. *Science*. 325: 201-
336 4.
- 337 • Collins K, Mitchell JR. 2002. Telomerase in the human organism. *Oncogene* 21: 564-
338 79.
- 339 • Epstein ND, Karlsson S, O'Brien S, Modi W, Moulton A, Nienhuis AW. 1987. A new
340 moderately repetitive DNA sequence family of novel organization. *Nucleic Acids Res*
341 15: 2327-41.
- 342 • Flores SC, Sunnerhagen P, Moore TK, Gaubatz JW. 1988. Characterization of
343 repetitive sequence families in mouse heart small polydisperse circular DNAs: age-
344 related studies. *Nucleic Acids Res* 16:3889-906.
- 345 • Flores SC, Sunnerhagen P, Moore TK, Gaubatz JW. 1988. Characterization of
346 repetitive sequence families in mouse heart small polydisperse circular DNAs: age-
347 related studies. *Nucleic Acids Res* 16: 3889-906.
- 348 • Fritze CE, Verschueren K, Strich R, Easton Esposito R. 1997. Direct evidence for
349 SIR2 modulation of chromatin structure in yeast rDNA. *EMBO J* 16: 6495-509
- 350 • Froy O, Miskin R (2010) Effect of feeding regimens on circadian rhythms:
351 implications for aging and longevity. *Aging* 2:7-27.
- 352 • Gaubatz JW. 1990. Extrachromosomal circular DNAs and genomic sequence
353 plasticity in eukaryotic cells. *Mutat Res* 237: 271-92.
- 354 • Gonzalez IL, Sylvester JE. 1995. Complete sequence of the 43-kb human ribosomal
355 DNA repeat: analysis of the intergenic spacer. *Genomics* 27: 320-8.
- 356 • Gotta M, Strahl-Bolsinger S, Renauld H, Laroche T, Kennedy BK, Grunstein M,
357 Gasser SM. 1997. Localization of Sir2p: the nucleolus as a compartment for silent
358 information regulators. *EMBO J* 16: 3243-55.

- 359 • Gottlieb S, Esposito RE. 1989. A new role for a yeast transcriptional silencer gene,
360 SIR2, in regulation of recombination in ribosomal DNA. *Cell* 1989 56:771-6.
- 361 • Henderson AS, Warburton D, Atwood KC. 1972. Location of ribosomal DNA in the
362 human chromosome complement. *Proc Natl Acad Sci* 69:3394-8.
- 363 • Hochstrasser T, Marksteiner J, Humpel C. 2012. Telomere length is age-dependent
364 and reduced in monocytes of Alzheimer patients. *Exp Gerontol* 47:160-3.
- 365 • Howitz KT, Bitterman KJ, Cohen HY, Lamming DW, Lavu S, Wood JG, Zipkin RE,
366 Chung P, Kisielewski A, Zhang LL, Scherer B, Sinclair DA. 2003. Small molecule
367 activators of sirtuins extend *Saccharomyces cerevisiae* lifespan. *Nature* 425:191-6.
- 368 • Hubbard BP, Gomes AP, Dai H, Li J, Case AW, Considine T, Riera TV, Lee JE, E SY,
369 Lamming DW, Pentelute BL, Schuman ER, Stevens LA, Ling AJ, Armour SM, Michan
370 S, Zhao H, Jiang Y, Sweitzer SM, Blum CA, Disch JS, et al. 2013. Evidence for a
371 common mechanism of SIRT1 regulation by allosteric activators. *Science* 339: 1216-
372 9.
- 373 • Jiang WQ, Zhong ZH, Henson JD, Neumann AA, Chang AC, Reddel RR. 2005.
374 Suppression of alternative lengthening of telomeres by Sp100-mediated
375 sequestration of the MRE11/RAD50/NBS1 complex. *Mol Cell Biol* 25: 2708-21.
- 376 • Jones RS, Potter SS. 1985. L1 sequences in HeLa extrachromosomal circular DNA:
377 evidence for circularization by homologous recombination. *Proc Natl Acad Sci* 82:
378 1989-93.
- 379 • Kohany O, Gentles AJ, Hankus L, Jurka J. 2006. Annotation, submission and
380 screening of repetitive elements in Repbase: Repbase Submitter and Censor
381 *Bioinformatics* 7: 474.
- 382 • Kouprina N, Mullokandov M, Rogozin IB, Collins NK, Solomon G, Otstot J, Risinger
383 JI, Koonin EV, Barrett JC, Larionov V. 2004. The SPANX gene family of cancer/testis-
384 specific antigens: rapid evolution and amplification in African great apes and
385 hominids. *Proc Natl Acad Sci* 101: 3077-82.
- 386 • Lam YY, Peterson CM, Ravussin E. 2013. Resveratrol vs. calorie restriction: Data
387 from rodents to humans. *Exp Gerontol* 48: 1018-24.
- 388 • Little RD, Braaten DC. 1989. Genomic organization of human 5 S rDNA and
389 sequence of one tandem repeat. *Genomics* 4: 376-83.
- 390 • Mair W, Dillin A. 2008. Aging and survival: the genetics of life span extension by
391 dietary restriction. *Annu Rev Biochem* 77: 727-54.
- 392 • Mangialasche F, Kivipelto M, Solomon A, Fratiglioni L. 2012. Dementia prevention:
393 current epidemiological evidence and future perspective. *Alzheimers Res Ther* 4: 6.

- 394 • McEachern MJ, Krauskopf A, Blackburn EH. 2000. Telomeres and their control. *Annu*
395 *Rev Genet* 34: 331-358.
- 396 • Meyerink JH, Klootwijk J, Planta RJ, van der Ende A, van Bruggen EF. 1979.
397 Extrachromosomal circular ribosomal DNA in the yeast *Saccharomyces*
398 *carlsbergensis*. *Nucleic Acids Res* 7:69-76.
- 399 • Minamino T, Miyauchi H, Yoshida T, Komuro I. 2003. Endothelial cell senescence in
400 human atherosclerosis: role of telomeres in endothelial dysfunction. *J Cardiol* 41:39-
401 40.
- 402 • Murayama A, Ohmori K, Fujimura A, Minami H, Yasuzawa-Tanaka K, Kuroda T, Oie
403 S, Daitoku H, Okuwaki M, Nagata K, Fukamizu A, Kimura K, Shimizu T, Yanagisawa
404 J. 2008. Epigenetic control of rDNA loci in response to intracellular energy status.
405 *Cell* 2008 133: 627-39.
- 406 • Palacios JA, Herranz D, De Bonis ML, Velasco S, Serrano M, Blasco MA. 2010.
407 SIRT1 contributes to telomere maintenance and augments global homologous
408 recombination. *J Cell Biol* 191: 1299-313.
- 409 • Riabowol K, Shmookler Reis RJ, Goldstein S. 1985. Interspersed repetitive and
410 tandemly repetitive sequences are differentially represented in extrachromosomal
411 covalently closed circular DNA of human diploid fibroblasts. *Nucleic Acids Res* 13:
412 5563-84.
- 413 • Savale L, Chaouat A, Bastuji-Garin S, Marcos E, Boyer L, Maitre B, Sarni M, Housset
414 B, Weitzenblum E, Matrat M, Le Corvoisier P, Rideau D, Boczkowski J, Dubois-
415 Randé JL, Chouaid C, Adnot S. 2009. Shortened telomeres in circulating leukocytes
416 of patients with chronic obstructive pulmonary disease. *Am J Respir Crit Care Med*
417 179: 566-71.
- 418 • Shibata Y, Kumar P, Layer R, Willcox S, Gagan JR, Griffith JD, Dutta A. 2012.
419 Extrachromosomal microDNAs and chromosomal microdeletions in normal tissues.
420 *Science* 336: 82-6.
- 421 • Sinclair DA, Guarente L. 1997. Extrachromosomal rDNA circles--a cause of aging in
422 yeast. *Cell* 91:1033-42.
- 423 • Smit AF. 1999. Interspersed repeats and other mementos of transposable elements
424 in mammalian genomes. *Curr Opin Genet Dev* 9: 657-63.
- 425 • Song T, Yang L, Kabra N, Chen L, Koomen J, Haura EB, Chen J. 2013. The NAD+
426 synthesis enzyme nicotinamide mononucleotide adenylyltransferase (NMNAT1)
427 regulates ribosomal RNA transcription. *J Biol Chem* 288: 20908-17.
- 428 • Sorensen PD, Frederiksen S. 1991. Characterization of human 5S rRNA genes.
429 *Nucleic Acids Res* 19: 4147-5.

- 430 • Stults DM, Killen MW, Pierce HH, Pierce AJ. 2008. Genomic architecture and
431 inheritance of human ribosomal RNA gene clusters. *Genome Res* 18: 13-8.
- 432 • Suh JH, Sieglaff DH, Zhang A, Xia X, Cvorov A, Winnier GE, Webb P. 2013. SIRT1 is
433 a Direct Coactivator of Thyroid Hormone Receptor β 1 with Gene-Specific Actions.
434 *PLoS One* 8: e70097.
- 435 • Torres G, Frisella PD, Yousuf SJ, Sarwar S, Baldinger L, Zakhary SM, Leheste JR.
436 2008. A ChIP-cloning approach linking SIRT1 to transcriptional modification of DNA
437 targets. *Biotechniques* 44: Pxi-Pxii.
- 438 • Torres G, Dileo JN, Hallas BH, Horowitz JM, Leheste JR. 2011. Silent information
439 regulator 1 mediates hippocampal plasticity through presenilin1. *Neuroscience*
440 179:32-40.
- 441 • Viret JF, Bravo A, Alonso JC. 1991. Recombination-dependent concatemeric plasmid
442 replication. *Microbiol Rev* 55: 675-83.
- 443 • Wachtler F, Schöfer C, Schedle A, Schwarzacher HG, Hartung M, Stahl A, Gonzales
444 I, Sylvester J. 1991. Transcribed and nontranscribed parts of the human ribosomal
445 gene repeat show a similar pattern of distribution in nucleoli. *Cytogenet Cell Genet*
446 57: 175-8.
- 447 • Wu Q, Maniatis T. 1999. A striking organization of a large family of human neural
448 cadherin-like cell adhesion genes. *Cell* 97: 779-90.
- 449 • Yang L, Song T, Chen L, Kabra N, Zheng H, Koomen J, Seto E, Chen J. 2013.
450 Regulation of SirT1-NML binding by rRNA coordinates ribosome biogenesis with
451 nutrient availability. *Mol Cell Biol* 33: 3835-48.
- 452 • Zellinger B, Akimcheva S, Puizina J, Schirato M, Riha K. 2007. Ku suppresses
453 formation of telomeric circles and alternative telomere lengthening in Arabidopsis.
454 *Mol Cell* 27: 163-9.

1

Figure 1

Figure 1 Resveratrol treatment induces the expression of *sirt1* and rDNA genes and does not alter Alu-eccDNA in HEK-293 cells. **A)** QPCR-analysis reveals increases in relative gene expression for *sirt1* (1.9-fold), *rna45s5* (1.8-fold) and *rn5s1* (3.5-fold) with resveratrol (R) treatment (50 μ M in DMSO, 48h) compared to control (C) conditions (DMSO). **B)** The same treatment has no significant effect on Alu-eccDNA in either nuclear or cytoplasmic compartments of HEK-293 cells. The relative Alu-eccDNA index compares Alu-eccDNA with β -actin expression of the same treatment group via QPCR. Values are means \pm SEM. * indicates statistical significance of annotated P; n = 20 for all groups.

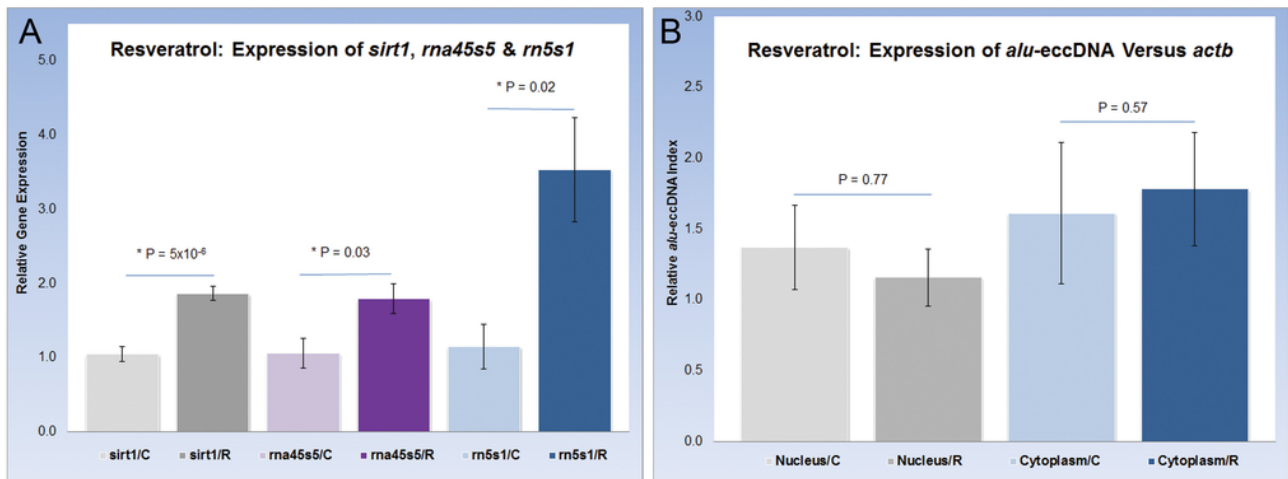


Figure 2

Figure 2 Resveratrol treatment significantly increases cytoplasmic rn5s1-eccDNA in human cells. QPCR analysis (relative to Alu-eccDNA) comparing resveratrol (R) treatment (50 μ M in DMSO, 48h) with control (C) conditions (DMSO) reveals significantly increased rn5s1-eccDNA in the cytoplasm of **A.** HEK-293 cells (2.2-fold), **B.** MCF7 cells (3.4-fold) and **C.** SH-SY5Y cells (1.5-fold). Concomitantly, rn5s1-eccDNA decreases significantly (-60%) in HEK-293 cells nuclei but not in other cells. **D.** Southern-blot using a gene-specific, labeled DNA probe confirms rn5s1eccDNA in HEK-293 cells (λ). Cytoplasmic and nuclear eccDNA extracts are linearized (sonication or BamHI), electrophoresed and blotted. Lower bands are consistent with 2.2kb rn5s1eccDNA monomers. Only cytoplasmic samples display an additional signal around 12kb consistent with rn5s1eccDNA multimers. QPCR-values are means \pm SEM. * indicates statistical significance of annotated P; n = 20 per group (**A-C**).

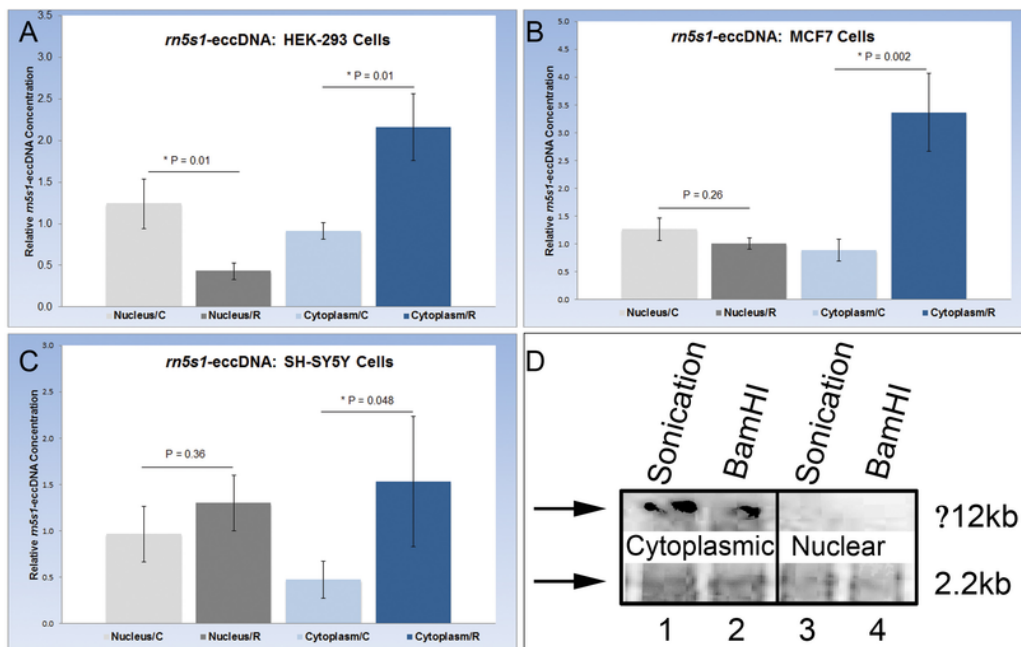
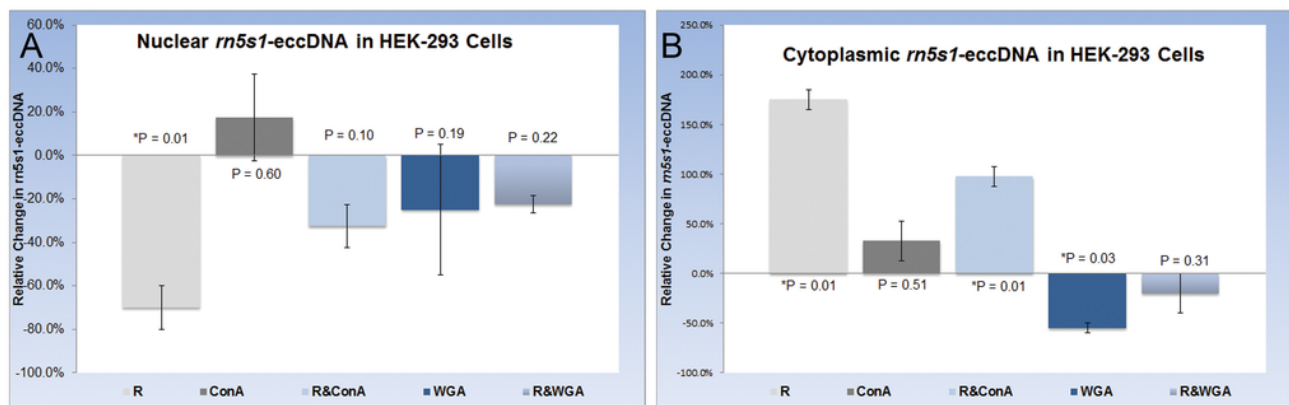


Figure 3

Figure 3 Increases in cytoplasmic r5s1-eccDNA in HEK-293 cells involve nuclear transport. QPCR analysis (relative to Alu-eccDNA) of r5s1-eccDNA under various conditions relative to untreated controls (baseline). Chemical reagents used: Resveratrol (R); concavalin A (ConA; control lectin); wheat germ agglutinin (WGA; nuclear transport inhibitor). **A.** Nuclear extracts show a significant resveratrol-dependent r5s1-eccDNA reduction (-70%; R) which is WGA-sensitive (-20%; R&WGA). **B.** With resveratrol, cytoplasmic r5s1-eccDNA surges (+180% R; +100% R&ConA) and returns to baseline with WGA (R&WGA). WGA by itself reduces baseline levels of r5s1-eccDNA significantly (-50%). Values are means \pm SEM. * indicates statistical significance of annotated P; n = 12 per group.



4

Figure 4

Figure 4. HEK-293 cells display genome-wide formation of eccDNA. This flowchart identifies the different types of eccDNA found in HEK-293 cells and classifies short repetitive DNA elements included. Our novel isolation and cloning strategy identified 48 eccDNA clones of which 13 map to coding genes (see Table 1). The majority of the non-mitochondrial clones (31 with tandem repeats and 3 with unique sequences) contain 1-4 short repetitive DNA elements (with an average of 1.7) possibly responsible for their mobilization. The majority (91%) encode transposable elements with class-I retrotransposons (94%; LINE, SINE, ERV and Alu elements) being dominant over class-II DNA transposons (6%; hAT). The minority (9%) includes interspersed repeats such as *alus* and *aluj*.

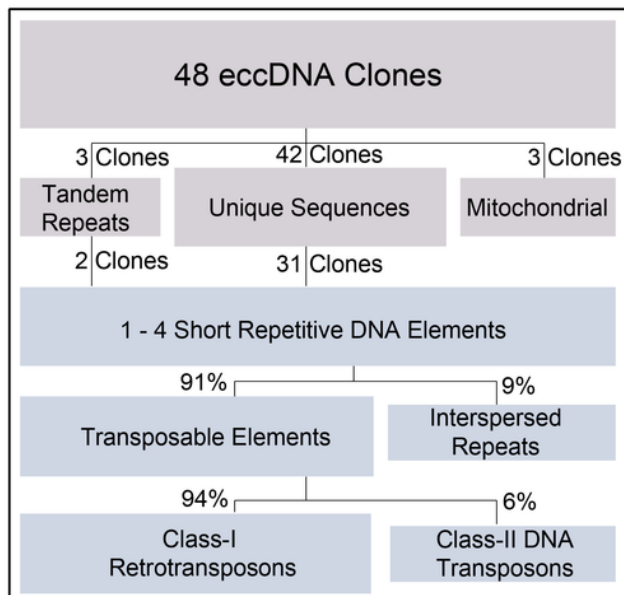


Table 1 (on next page)

Table 1

Table 1 Identification and characterization of eccDNA linked to specific genes. Overlapping exons (ex) and introns (int) are sequentially numbered and the upstream (5') position of the untranslated region (utr) in rn5S1 is indicated. Genes and repetitive elements are abbreviated according to standard convention. Other abbreviations: SINE: short interspersed nuclear elements; hAT: a class-II DNA transposon superfamily; LINE: long interspersed nuclear elements; ERV: endogenous retrovirus; IR: Interspersed repeat.

Gene	Chromosome	Contains	Process Involvement	Size [bp]	Repetitive Element
<i>acp6</i>	1	int2	mitochondrial lipid biosynthesis	598	<i>aluSc</i> (SINE); <i>mer5A1</i> (hAT)
<i>cdh9</i>	5	int5	promotes cell-to-cell adhesion	650	<i>l1hS</i> (LINE); <i>lipmA2</i> (LINE)
<i>snx24</i>	5	int3	vesicular membrane transport	761	<i>herM</i> (ERV)
<i>aldh3a2</i>	17	ex3-int3	fatty alcohol oxidation	481	-
<i>bicD1</i>	12	int2	cytoskeleton-based RNA sorting	781	<i>aluS</i> (IR); <i>l1me1</i> (LINE)
<i>cpE</i>	4	int1	neurotransmitter & peptide hormone production	700	<i>l1mb8</i> (LINE)
<i>lacc1</i>	13	int2	leprocy & Crohn's disease	560	<i>aluJb</i> (SINE)
<i>nfyb</i>	12	int6	transcription factor (repressor)	460	<i>aluJo</i> (SINE)
<i>parva</i>	11	int1	kidney development; F-actin binding	672	-
<i>pcdha1</i>	5	int3	neuronal cell-cell interaction	870	-
<i>plekhm3</i>	2	int1	intracellular signal transduction	437	<i>aluJo</i> (SINE)
<i>rn5S1</i>	1	5'utr	ribosomal & mitochondrial function	661	<i>hervip10fh</i> (ERV)
<i>sash1</i>	6	int19-ex20	tumor suppression	629	-
<i>specc1</i>	17	int3	structural function	737	<i>lipA8</i> (LINE)
<i>spy1</i>	7	int3	cell-cycle regulation	708	<i>aluJ</i> (IR); <i>aluJo</i> (SINE)
<i>tdrd7</i>	9	ex20-ex21	lens development	633	-